

Supporting Information for

Evaluating $\text{Ce}^{3+} \rightarrow \text{Tb}^{3+} \rightarrow \text{Eu}^{3+}$ cascade sensitization in
 $\text{LiSrY}_2(\text{BO}_3)_3$ for near-UV excited white emission

Xining Chen, Rihong Cong, Tao Yang**

College of Chemistry and Chemical Engineering, Chongqing University, Chongqing

401331, People's Republic of China

*Corresponding authors: congrihong@cqu.edu.cn; taoyang@cqu.edu.cn

Table S1. Cell lattice parameters (a , c , V) for $\text{LiSr}(\text{Y}_{0.99-x}\text{Ce}_{0.01}\text{Tb}_x)_2(\text{BO}_3)_3$ ($0 \leq x \leq$

0.60) obtained from Le Bail fitting on the powder XRD (space group $P\bar{3}m1$)

x	a (Å)	c (Å)	V (Å ³)
$\text{LiSrY}_2(\text{BO}_3)_3$	10.326456(3)	6.387026(3)	590.84(4)
0	10.328750(4)	6.389453(3)	590.32(5)
0.01	10.334310(2)	6.395179(3)	591.49(4)
0.02	10.337464(6)	6.399243(3)	592.23(1)
0.03	10.344801(1)	6.405210(2)	593.62(2)
0.04	10.349964(3)	6.407862(3)	594.46(4)
0.05	10.356403(4)	6.413693(5)	595.74(6)
0.06	10.360590(1)	6.418460(3)	596.67(4)

Table S2. Cell lattice parameters (a , c , V) for $\text{LiSr}(\text{Y}_{0.993-m-n}\text{Ce}_{0.007}\text{Tb}_m\text{Eu}_n)_2(\text{BO}_3)_3$ ($0 \leq$

$m \leq 0.02$, $0 \leq n \leq 0.04$) obtained from Le Bail fitting on the powder XRD (space group

$P\bar{3}m1$)

m	n	a (Å)	c (Å)	V (Å ³)
0	0	10.328010(1)	6.390140(1)	590.30(2)
0.02	0.005	10.329016(6)	6.390909(3)	590.49(2)
0.02	0.01	10.329100(3)	6.391699(4)	590.57(2)
0.02	0.02	10.330510(2)	6.392964(2)	590.85(3)
0.02	0.03	10.331688(2)	6.393253(4)	591.01(2)
0.02	0.04	10.332250(3)	6.395097(3)	591.25(4)

0.01	0.002	10.328550(1)	6.390289(8)	590.38(1)
0.01	0.005	10.329057(4)	6.390620(8)	590.47(1)
0.005	0.005	10.329118(2)	6.389454(1)	590.37(3)
0.005	0.01	10.329646(2)	6.389998(2)	590.48(3)

Table S3. Average fluorescence decay lifetime (τ) using double exponential function fitting and so-calculated energy transfer efficiency (η_{ET}) for $\text{LiSr}(\text{Y}_{0.99-x}\text{Ce}_{0.01}\text{Tb}_x)_2(\text{BO}_3)_3$ ($0 \leq x \leq 0.60$)

x	A_1	τ_1 (ns)	A_2	τ_2 (ns)	τ (ns)	$\eta_{ET} = 1 - \tau/\tau_0$ (%)
0	9.81E+04	4.19278	7605.16665	11.98687	5.61	
0.10	9.22E+06	2.40301	5928.22139	10.69056	2.43	56.72
0.20	2.35E+07	2.19643	5900.16438	9.14023	2.20	60.69
0.30	5.79E+07	2.01103	4635.52287	8.43517	2.01	64.09
0.40	9.70E+07	1.88984	2475.33818	8.11577	1.89	66.28
0.50	7.38E+08	1.57545	1745.14793	7.66754	1.58	71.90
0.60	9.87E+12	0.93746	1545.96071	7.04652	0.94	83.28

Table S4. The room-temperature CIE chromaticity coordinates of $\text{LiSr}(\text{Y}_{0.99-x}\text{Ce}_{0.01}\text{Tb}_x)_2(\text{BO}_3)_3$ ($0 \leq x \leq 0.60$) phosphors

x	EX (nm)	CIE x	CIE y
0	335	0.1602	0.0217
0.10	335	0.2485	0.5005

0.20	335	0.2593	0.5464
0.30	335	0.2617	0.5568
0.40	335	0.2674	0.5646
0.50	335	0.2638	0.5637
0.60	335	0.2646	0.5630
$\text{LiSr}(\text{Y}_{0.80}\text{Tb}_{0.20})_2(\text{BO}_3)_3$	260	0.2461	0.5672

Table S5. The temperature-dependent CIE chromaticity coordinates of $\text{LiSr}(\text{Y}_{0.79}\text{Ce}_{0.01}\text{Tb}_{0.2})_2(\text{BO}_3)_3$ phosphors

Temperature(K)	EX (nm)	CIE x	CIE y
303	335	0.2593	0.5464
333	335	0.2579	0.5483
363	335	0.2583	0.5488
393	335	0.2585	0.5484
423	335	0.2574	0.5500
453	335	0.2564	0.5504
483	335	0.2569	0.5504

Table S6. Average fluorescence decay lifetime (τ) using double exponential function fitting and so-calculated energy transfer efficiency (η_{ET}) for $\text{LiSr}(\text{Y}_{0.995}\text{Tb}_{0.005})_2(\text{BO}_3)_3$, $\text{LiSr}(\text{Y}_{0.985}\text{Tb}_{0.005}\text{Eu}_{0.01})_2(\text{BO}_3)_3$

	A_1	τ_1 (ns)	A_2	τ_2 (ns)	τ (ns)	$\eta_{ET} = 1 - \tau/\tau_0$ (%)
$\text{LiSr}(\text{Y}_{0.995}\text{Tb}_{0.005})_2(\text{BO}_3)_3$	2359.1111	2.7759	2702.9163	2.4058	2.59	
$\text{LiSr}(\text{Y}_{0.985}\text{Tb}_{0.005}\text{Eu}_{0.01})_2(\text{BO}_3)_3$	2981.2782	2.7668	2421.5485	1.9537	2.47	4.67%

Table S7. The room-temperature CIE chromaticity coordinates of $\text{LiSr}(\text{Y}_{0.993-m-n}\text{Ce}_{0.007}\text{Tb}_m\text{Eu}_n)_2(\text{BO}_3)_3$ ($0.005 \leq m \leq 0.02$, $0.002 \leq n \leq 0.04$) phosphors

m	n	EX (nm)	CIE x	CIE y	CCT(K)
0.02	0.005	335	0.3418	0.4643	
0.02	0.01	335	0.3548	0.4723	
0.02	0.02	335	0.3788	0.4756	
0.02	0.03	335	0.4058	0.4690	
0.02	0.04	335	0.4218	0.4713	
0.01	0.002	335	0.3063	0.3941	
0.01	0.005	335	0.3168	0.4052	
0.005	0.005	335	0.2957	0.3398	
0.005	0.01	335	0.3030	0.3351	6989

Table S8. Comparison of key luminescence performance parameters of the present $\text{LiSrY}_2(\text{BO}_3)_3: \text{Ce}^{3+}/\text{Tb}^{3+}/\text{Eu}^{3+}$ phosphor with other reported single-phase white-emitting phosphors

Phosphor System	CIE (x, y)	CCT (K)	CRI	IQE (%)	Thermal stability (@423K)	Ref.
$\text{LiSrY}_2(\text{BO}_3)_3$ ($\text{Ce}^{3+}/\text{Tb}^{3+}/\text{Eu}^{3+}$)	(0.3030, 0.3351)	6989	84	5.90	60.47%	This work
YBO_3 ($\text{Ce}^{3+}/\text{Tb}^{3+}/\text{Eu}^{3+}$)	(0.318, 0.337)	—	—	—	—	1
$\text{Y}_2\text{Si}_2\text{O}_7$ ($\text{Ce}^{3+}/\text{Tb}^{3+}/\text{Eu}^{3+}$)	(0.327, 0.327)	—	85	69	—	2
$\text{Ca}_2\text{MgSi}_2\text{O}_7$ ($\text{Ce}^{3+}/\text{Tb}^{3+}/\text{Eu}^{3+}$)	(0.345, 0.312)	4804	—	45.1	—	3
$\text{Ca}_3\text{Gd}(\text{GaO})_3(\text{BO}_3)_4$ ($\text{Ce}^{3+}/\text{Tb}^{3+}/\text{Eu}^{3+}$)	(0.346, 0.475)	—	—	—	55.5%	4
NaGdF_4 ($\text{Ce}^{3+}/\text{Tb}^{3+}/\text{Eu}^{3+}$)	(0.32, 0.32)	—	—	—	—	5
$\text{Na}_5\text{Y}_9\text{F}_{32}$ ($\text{Ce}^{3+}/\text{Tb}^{3+}/\text{Eu}^{3+}$)	(0.299, 0.321)	7434	—	15.32	89%	6
$\text{Na}_{1.5}\text{Y}_{2.5}\text{F}_9$ ($\text{Ce}^{3+}/\text{Tb}^{3+}/\text{Eu}^{3+}$)	(0.311, 0.347)	6467.72	—	—	57.6%	7
$\text{LiY}_6\text{O}_5(\text{BO}_3)_3$ ($\text{Bi}^{3+}/\text{Tb}^{3+}/\text{Eu}^{3+}$)	(0.323, 0.339)	5903	85	5.67	64.5%	8

NaYGeO ₄ (Bi ³⁺ /Tb ³⁺ /Eu ³⁺)	(0.336, 0.296)	5205	—	—	~60%	9
LaInO ₃ (Bi ³⁺ /Tb ³⁺ /Eu ³⁺)	(0.325, 0.303)	—	—	—	—	10

References.

1. S. Kang, Z. K. Yu, Q. R. Tian, M. H. Tai, J. Y. Wang, D. L. Jin, L. C. Wang, *Electron. Mater. Lett.*, 2022, **18**, 540–546.
2. J. Sokolnicki, *J. Lumin.*, 2013, **134**, 600–606.
3. C. W. Ye, *J. Lumin.*, 2019, **213**, 75–81.
4. B. Li, X. Y. Huang, *Ceram. Int.*, 2018, **44**, 4915–4923.
5. J. Liang, T. Fan, J. T. Lu, T. J. Guan, T. T. Deng, B. Y. Xiong, *RSC Adv.*, 2023, **13**, 25681–25690.
6. L. Z. Fang, X. Zhou, H. P. Xia, H. W. Song, B. J. Chen, *Solid State Commun.*, 2022, **357**, 114969.
7. Z. Niu, Q. L. Li, B. C. Yu, Y. Jiang, X. Y. Cai, Y. P. Zhang, *Ceram. Int.*, 2023, **49**, 12540–12550.
8. L. Xiong, T. Yang, R. H. Cong, *J. Solid State Chem.*, 2025, **350**, 125504.
9. E. L. Wang, K. Feng, J. Li, X. D. Zhou, X. K. Sun, *J. Lumin.*, 2022, **250**, 119108.
10. X. W. Hu, F. Piccinelli, M. Bettinelli, *J. Alloys Compd.*, 2022, **899**, 163344.

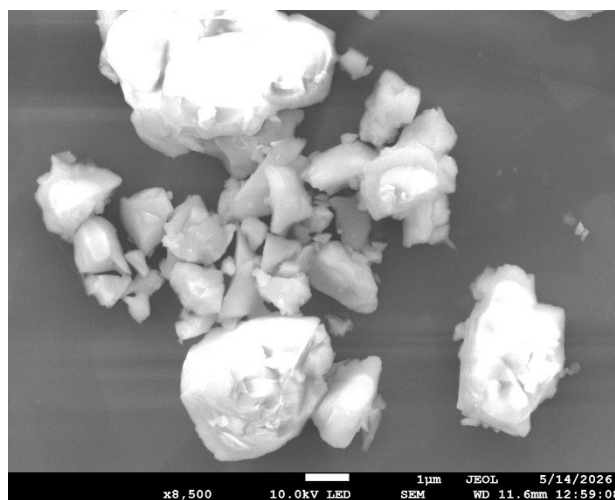


Figure S1. SEM image of $\text{LiSr}(\text{Y}_{0.978}\text{Ce}_{0.007}\text{Tb}_{0.005}\text{Eu}_{0.01})_2(\text{BO}_3)_3$.

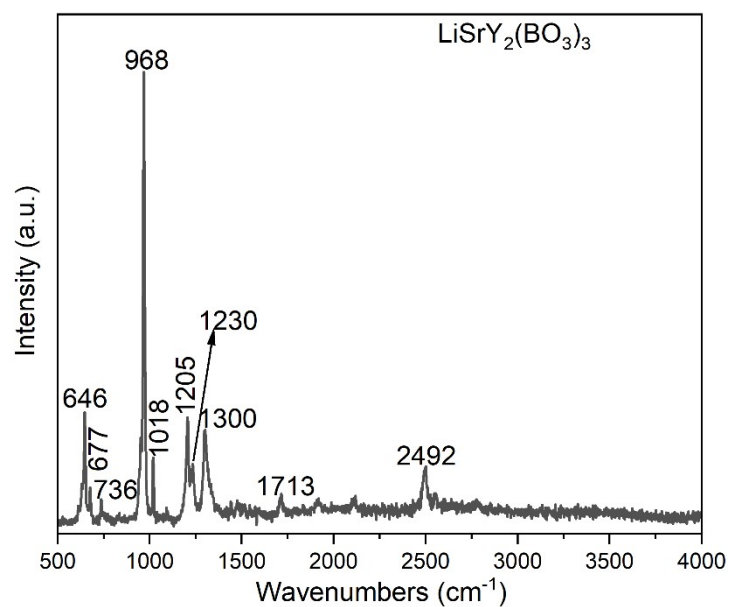


Figure S2. Raman spectrum of $\text{LiSrY}_2(\text{BO}_3)_3$.

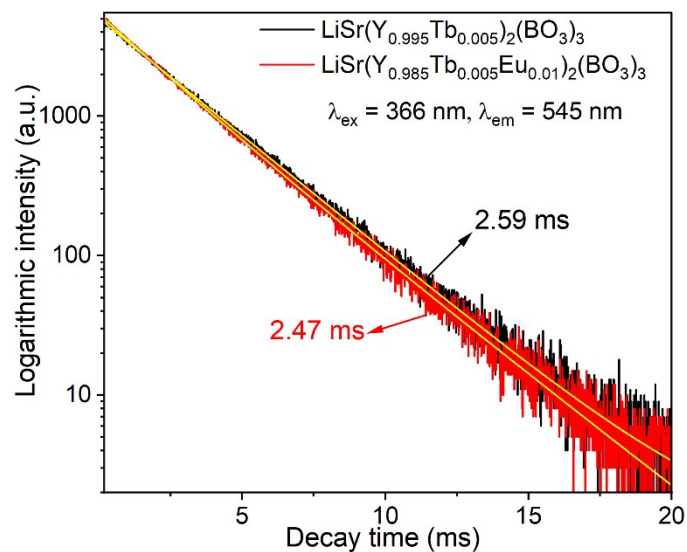


Figure S3. Fluorescent decay curves of Tb^{3+} in $\text{LiSr}(\text{Y}_{0.995}\text{Tb}_{0.005})_2(\text{BO}_3)_3$ and $\text{LiSr}(\text{Y}_{0.985}\text{Tb}_{0.005}\text{Eu}_{0.01})_2(\text{BO}_3)_3$.

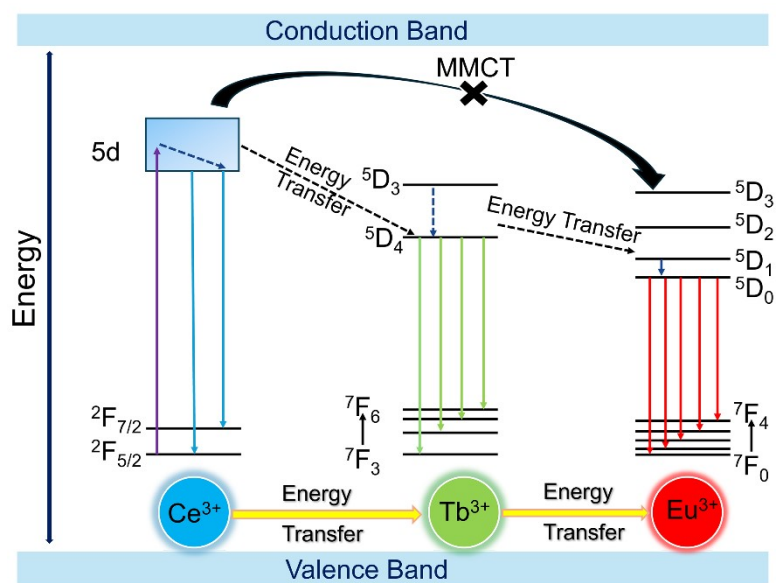


Figure S4. Illustration of energy levels of Ce^{3+} , Tb^{3+} , Eu^{3+} ions and $\text{Ce}^{3+} \rightarrow \text{Tb}^{3+} \rightarrow \text{Eu}^{3+}$ energy transfer mechanism.